Acta Crystallographica Section A
Foundations of Crystallography
ISSN 0108-7673

Received 22 March 2012
Accepted 23 July 2012

Is it possible to derive quantitative information on polarization of electron density from the multipolar model?

Joanna Maria Bąk,[a] Żaneta Czyżnikowska[b] and Paulina Maria Dominiak[a]*

[a]Department of Chemistry, University of Warsaw, ul. Pasteura 1, 02-093 Warszawa, Poland, and [b]Department of Inorganic Chemistry, Wroclaw Medical University, Szewska 38, 50-139 Wroclaw, Poland. Correspondence e-mail: pdomin@chem.uw.edu.pl

The accuracy of electrostatic properties estimated from the Hansen–Coppens multipolar model was verified. Tests were carried out to determine whether the multipolar model is accurate enough to study changes of electrostatic properties under the influence of a crystal field. Perturbed and unperturbed electron densities of individual molecules of amino acids and dipeptides were obtained from cluster and perturbation theory calculations. This enabled the changes in electrostatic properties values caused by polarization of the electron density to be characterized. Multipolar models were then fitted to the subsequent theoretical electron densities. The study revealed that electrostatic properties obtained from the multipolar models are significantly different from those obtained directly from the theoretical densities. The electrostatic properties of isolated molecules are reproduced better by multipolar models than the electrostatic properties of molecules in a crystal. Changes of electrostatic properties caused by perturbation of electron density due to the crystal environment are barely described by the multipolar model. As a consequence, the electrostatic properties obtained from multipolar models fitted to the perturbed theoretical densities derived either from cluster or periodic calculations do not differ much from those estimated from multipolar models fitted to densities of isolated molecules. The main reason for this seems to be related to an inadequate description of electron-density polarization in the vicinity of the nuclei by the multipolar model.

1. Introduction

Calculations of electrostatic properties of biomolecules or crystal energy landscapes are a particular challenge to computational chemistry. Although periodic and accurate *ab initio* methods are being developed for such calculations, they are computationally very expensive. In turn, applying traditional force fields for organic systems may be fast, but it is too basic to model intra- and intermolecular forces with sufficient accuracy. Therefore, we face a need for alternative models, which should be quite simple and capable of describing the aspherical electron density of molecules in a crystal.

The Hansen–Coppens multipolar model (HC-MM; Hansen & Coppens, 1978) was invented to enable refinement of electron density from X-ray diffraction data. In the HC-MM the electron density of a crystal is defined as a superposition of aspherical electron densities of atoms (pseudoatoms) constituting a crystal. Each pseudoatom is expressed as a sum of the spherical density of core electrons and an atom-centred multipolar expansion describing the distribution of valence electrons. In the model, the core density is kept unrefined whereas population and contraction–expansion parameters of the multipolar functions can be refined against experimental or theoretical structure factors. The HC-MM has been repeatedly used to study experimental electron density, as well as to obtain the electrostatic properties of given molecules in crystal environments (Destro *et al.*, 2008; Madsen *et al.*, 2000; Fournier *et al.*, 2009; Grabowsky *et al.*, 2008). The transferability of pseudoatom electron densities between different molecules in the HC-MM made possible a relatively easy standardization of parameters that describe the density of pseudoatoms with similar chemical environments. This led to the creation of databases of aspherical pseudoatom parameters (verification of the databases is summarized by Bąk *et al.*, 2011). These parameters can be used to build transferable aspherical atom models (TAAMs) to model the electron densities of a crystal. It was shown that a TAAM can be used instead of a conventional independent atom model in structural refinement of organic compounds and proteins (Zarychta *et al.*, 2007; Dittrich *et al.*, 2008; Volkov *et al.*, 2007), and to obtain approximated electrostatic properties of molecules in a crystal environment (*e.g.* Dominiak *et al.*, 2009).

Koritsanszky *et al.* (2010) showed that radial functions used in the HC-MM in multipolar expansion of pseudoatom electron densities are not flexible enough to describe electron density, especially in the vicinity of the nuclei. They introduced new radial functions fitted to theoretical electron densities of isolated molecules. They suggested using these theoretical models of electron density in multipolar refinement. However, the new radial functions have not yet been introduced to any software which enables such a refinement. Alternatively, the electrostatic properties of molecules in crystals can also be obtained from X-ray-constrained Hartree–Fock wavefunctions (Jayatilaka *et al.*, 2009).

Nevertheless, the number of publications focused on properties obtained from the HC-MM of theoretical or experimental electron densities still increases (Liebschner *et al.*, 2009; Hathwar *et al.*, 2011; Holstein *et al.*, 2010; Munshi *et al.*, 2010). The accuracy of such electrostatic properties is usually not discussed in the papers. Moreover, it is debatable whether the HC-MM is able to describe the polarization effect (Coppens *et al.*, 1984; Dovesi *et al.*, 1990; Spackman & Byrom, 1996; Spackman *et al.*, 1999; Dittrich *et al.*, 2012; Chambrier *et al.*, 2011).

Taking the above facts into account, we performed a systematic analysis of the electrostatic properties of a molecule estimated from the HC-MM of the crystal electron density. We verified the accuracy of the electrostatic properties obtained from the HC-MM fitted to theoretical electron densities, of either perturbed or isolated molecules, by referring them to the results obtained directly from the corresponding theoretical densities. On the basis of theoretical calculations we characterized changes of electrostatic properties due to electronic polarization. Then we tested whether the accuracy of the HC-MM is good enough to study changes of the electrostatic properties caused by the crystal environment. We obtained theoretical perturbed electron densities of individual molecules from cluster calculations. In the calculations the perturbation of the molecular density was induced by a cluster of atomic charges, dipoles and quadrupoles surrounding the central molecule, so as to simulate the influence of the crystal environment. A similar method for perturbing electron density was applied by Dittrich *et al.* (2012) for studying interaction densities. Their study indicated that theoretical interaction densities obtained from such cluster calculations reproduce well interaction densities obtained from theoretical periodic calculations. Perturbed and isolated-molecule theoretical densities were calculated on the basis of the same crystal geometries of a few amino acids and dipeptides. The comparison of the Coulombic electrostatic interaction energies obtained directly from the perturbed theoretical densities with the results of density fitting–density functional theory–symmetry adapted perturbation theory (DF–DFT–SAPT) calculations (Hesselmann *et al.*, 2005) made it possible to further verify the perturbation method.

We focused on interaction electron-density maps, dipole-moment vectors and Coulombic electrostatic energies of the interaction between two electron densities of individual molecules, which were placed as found in crystal geometries. The analyses enabled us to check whether quantitative information about the influence of the crystal environment on the electrostatic properties could be derived from multipolar models of crystal electron densities.

2. Theoretical calculations and multipolar refinement

2.1. DF–DFT–SAPT calculations

DF–DFT–SAPT calculations (Hesselmann *et al.*, 2005) were carried out for the total energy of interactions in dimers of amino acids. Interaction energies were obtained for 17 dimers, which were found in the crystal structures of: L-alanine (marked as ALA), L-His–L-Ala dihydrate (marked as HA), D,L-histidine (marked as HIS) and Gly–L-His dihydrate (marked as GH; Fig. 1). The crystal geometries resulting from periodic geometry optimizations (Bąk *et al.*, 2011) were used for the purpose of the computations.

The calculations were performed using the cc-pVDZ basis set augmented with a set of diffuse functions and the PBE0AC exchange–correlation functional recommended by Hesselmann *et al.* (2005). The asymptotic correction was determined as a difference between the highest occupied molecular orbital (HOMO) energy of each monomer and the ionization potential obtained from the calculations of their neutral and ionized forms. The total intermolecular interaction energy is defined as the sum of the first- and the second-order energies plus the δHF term [equation (1)]

$$E_{\rm int} = E^1_{\rm pol} + E^1_{\rm ex} + E^2_{\rm ind} + E^2_{\rm ex-ind} + E^2_{\rm disp} + E^2_{\rm ex-disp} + \delta{\rm HF}(2). \quad (1)$$

The first-order energy includes electrostatic and exchange–repulsion contributions, while the second-order energy includes induction, exchange–induction, dispersion and exchange–dispersion contributions. The density-fitting procedure was used in order to reduce the computational costs of calculations. All DF–DFT–SAPT calculations were performed using the *Molpro* suite of programs (Werner *et al.*, 2006).

2.2. Theoretical electron densities

Theoretical electron densities of isolated molecules were obtained from single-point calculations carried out using the *TONTO* program (Jayatilaka & Grimwood, 2003), using the same crystal geometries as in the case of the DF–DFT–SAPT calculations. Calculations were performed using the DFT method with the BLYP (Becke, 1993; Lee *et al.*, 1988) potential and two different basis sets: DZP (Dunning, 1970; model marked as $\rm DZP_{isol}$) and cc-pVDZ (Dunning, 1989; model marked as $\rm cc\text{-}pVDZ_{isol}$). For all calculations a high-accuracy Becke grid was used and the convergence tolerance of the total energy was equal to 0.00001 hartree. Level shift and a damping factor were used in the first cycles of the calculations.

Then, perturbation of individual molecular electron density was induced in cluster calculations that simulated the crystal environment. The clusters consisted of atom charges, dipoles and quadrupoles centred at atomic positions of all molecules surrounding the central molecule within a radius of 15 Å.

Iterated values of charges, dipoles and quadrupoles were derived from the theoretical electron densities of the central molecule using the Hirshfeld atom partitioning scheme. The values of electrostatic moments in the clusters were changed until convergence was achieved. Perturbation caused by water molecules was neglected in the calculations of HA and GH densities. Two different models of perturbed electron densities were obtained: $DZP_{perturb}$ for all four molecules studied and cc-$pVDZ_{perturb}$ for ALA and HIS, using DZP and cc-pVDZ basis sets, respectively. The values of the Coulombic interaction energies obtained from $DZP_{perturb}$ for ALA and HIS crystal structures were closer to the referential values obtained from the DF–DFT–SAPT method than the results obtained from cc-$pVDZ_{perturb}$. We decided therefore to perform our extended analyses using only the $DZP_{perturb}$ model.

Electron-density maps and dipole moments were calculated directly from the theoretical electron densities using the *TONTO* program. Coulombic energies of interactions in dimers were calculated using successive pairs of electron densities of individual molecules. Computations were performed using the *SPDFG* program (Volkov, King & Coppens, 2006) on the basis of electron densities, of either perturbed or isolated molecules, positioned in relative orientations as found in crystal geometries. The energies obtained from isolated-molecule electron densities (denoted as Ees further in the text) are expected to reproduce the values of the electrostatic energy component (E^1_{pol}) from the DF–DFT–SAPT method, whereas the energies calculated on the basis of perturbed electron densities (denoted further as Ecs) are assumed to be a good approximation of the sum of the electrostatic (E^1_{pol}) and induction (E^2_{ind}) energy components from the DF–DFT–SAPT method.

Table 1
RMSDs calculated between Ees or Ecs (kJ mol^{-1}) energy values obtained from given theoretical models of electron densities or resulting from the SAPT calculations (Ees = E^1_{pol}, Ecs = $E^1_{pol} + E^2_{ind}$).

The statistics taking into account results obtained from ten dimers of ALA and HIS are given together with the ones based on 17 dimers of all four crystal structures (numbers in parentheses).

	Ecs SAPT	Ees DZP_{isol}	Ecs $DZP_{perturb}$	Ees cc-$pVDZ_{isol}$	Ecs cc-$pVDZ_{perturb}$
Ees SAPT	61 (64)	10 (11)	66 (73)	18 (21)	44
Ecs SAPT		70 (74)	28 (33)	77 (83)	29
Ees DZP_{isol}			74 (82)	9 (11)	52
Ecs $DZP_{perturb}$				82 (91)	22
Ees cc-$pVDZ_{isol}$					60

Dittrich *et al.* (2012) performed cluster calculations applying the same method as in our studies, but using only atomic charges and dipoles to build the cluster. They showed that interaction densities obtained from fully periodic calculations and from cluster calculations are comparable. Additionally, in the course of our work, we verified whether perturbed electron densities obtained from cluster calculations are accurate enough to quantitatively reproduce changes of electrostatic properties caused by the influence of the electron densities of surrounding molecules. Hence, we compared the Ees and Ecs values obtained directly from theoretical densities to the results of the DF–DFT–SAPT calculations. Since there were differences among methods used for calculations (variant functional and/or basis set, variant model of perturbation: single molecule in the dimer or several neighbouring molecules in the crystal lattice, lack of exact correspondence between Ecs–Ees and E^2_{ind} from definition, *etc.*), we did not aim to get exact conformity of the Ees and Ecs values resulting from these methods. Our results show that the Ees values calculated from unperturbed electron densities deviate slightly from the results of the DF–DFT–SAPT method. The root-mean-square difference (RMSD) calculated between the Ees obtained from the two methods is 10 and 18 kJ mol^{-1} for DZP and cc-pVDZ basis sets, respectively (see Table 1). The difference is not much higher than the difference caused by the use of the variant basis set for isolated-molecule density calculations, RMSD = 9 kJ mol^{-1}. Larger disagreement, as expected, is observed for the Ecs values, RMSD = 28 and 29 kJ mol^{-1} for DZP and cc-pVDZ, respectively (see Table

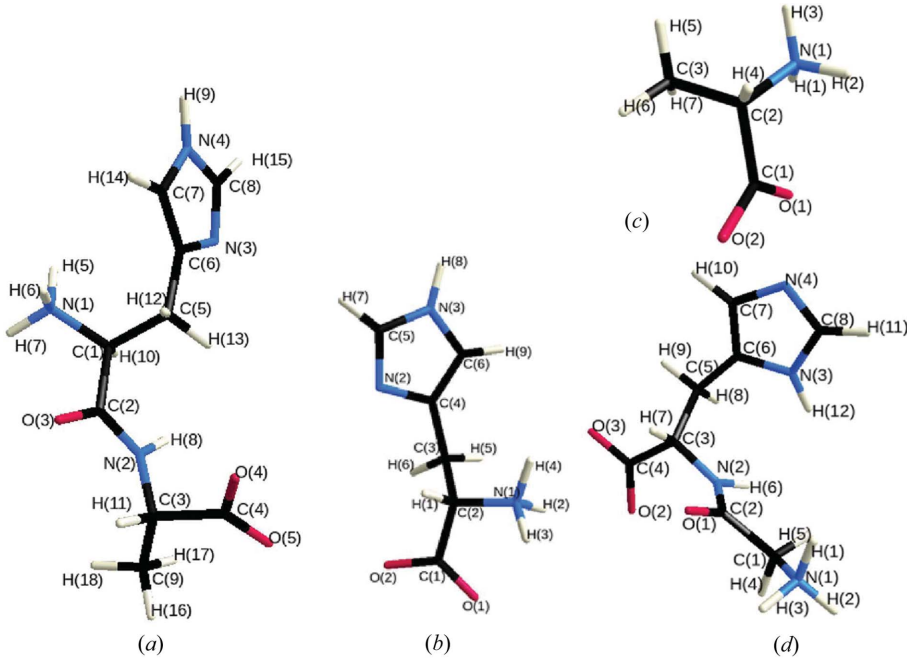

Figure 1
The molecular structures and labelling schemes of: (*a*) L-His–L-Ala (HA), (*b*) D,L-His (HIS), (*c*) L-Ala (ALA) and (*d*) Gly–L-His (GH).

1). Therefore we found it more appropriate to focus on the *shifts* that occurred between the Ees and Ecs values obtained using theoretical densities and check whether these are of the same magnitude as the values of induction (E^2_{ind} = Ecs − Ees) energy components from the DF–DFT–SAPT method. In spite of some dissimilarities in absolute values of Ees and Ecs, the cluster method used to perturb electron densities reproduces quite well shifts of Ecs values from corresponding values of Ees (see Fig. 2 and Table 1). The same trends can be seen in the results of cluster and DF–DFT–SAPT calculations. In both cases, the larger the electrostatic interaction energy Ees is, the larger is the shift of Ecs from Ees toward negative values. Moreover, the magnitude of the shifts is similar. The RMSD between Ees and Ecs energies is 61 kJ mol^{-1} for SAPT results as compared with 74 and 60 kJ mol^{-1} for cluster calculations with the use of the DZP or cc-pVDZ basis set, respectively. Thus we decided to apply the cluster perturbation method to study the influence of the crystal environment on electrostatic properties and to verify the ability of the multipolar model to reproduce such effects.

Table 2
List of acronyms used for electron density (ED) models.

	Unperturbed ED models	Perturbed ED models	Interaction ED models†
Theoretical electron densities	DZP_{isol} cc-$pVDZ_{isol}$	$DZP_{perturb}$ cc-$pVDZ_{perturb}$	DZP cc-pVDZ
Hansen–Coppens multipolar models of theoretical electron densities	MM_DZP_{isol} $MM\_cc\text{-}pVDZ_{isol}$	$MM\_DZP_{perturb}$ $MM\_cc\text{-}pVDZ_{perturb}$ CR	MM_DZP MM_cc-pVDZ

† Calculated by subtracting the electron-density models of the given isolated unperturbed molecules from the corresponding perturbed electron-density models.

2.3. Multipolar models of theoretical electron densities

Firstly, successive sets of theoretical structure factors were calculated on the basis of theoretical densities (DZP_{isol}, $DZP_{perturb}$, cc-$pVDZ_{isol}$, cc-$pVDZ_{perturb}$) up to the resolution $\sin\theta/\lambda$ = 1.2 Å^{-1}. Structure factors were calculated using the *TONTO* program (Jayatilaka & Grimwood, 2003), by placing the electron density of an individual molecule in the original crystal cell and transforming it by all symmetry operations of a given space group. Afterwards, multipolar models were refined on *F*, with the *XDLSM* module from the *XD2006* program (Volkov, Macchi *et al.*, 2006), against each set of structure factors. Multipoles up to the hexadecapolar level for non-H atoms, and bond-directed dipoles and quadrupoles for H atoms were refined together with individual κ and κ' parameters for each atom. Local atomic site symmetry constraints were applied to multipolar population parameters. We observed that relieving the symmetry constraints applied to multipolar population parameters did not significantly change the resulting electron densities (Figs. 3*b* and 3*c*) and the Ecs values. Atomic positions and scale factors were not refined. Atomic scattering factors were based on the atomic wavefunctions of Clementi & Roetti (1974). Single ξ exponents corresponding to weighted averages over the *s*- and *p*-shell values given by Clementi & Raimondi (1963) were used for the radial functions of the deformation part. As a result the corresponding multipolar models for each compound were obtained: MM_DZP_{isol}, $MM\_DZP_{perturb}$, $MM\_cc\text{-}pVDZ_{isol}$, $MM\_cc\text{-}pVDZ_{perturb}$.

The analyses were extended over multipolar models fitted to the theoretical electron densities of crystals, obtained from periodic calculations at the B3LYP/DZP level (denoted here as CR) taken from our previous work (Bąk *et al.*, 2011).

The *XDPROP* module of the *XD2006* package was used to calculate electron-density maps, dipole-moment vectors and Coulombic energies of interactions (Ees and Ecs) for dimers from the multipolar models of electron densities.

A list of all acronyms used for density models is given in Table 2.

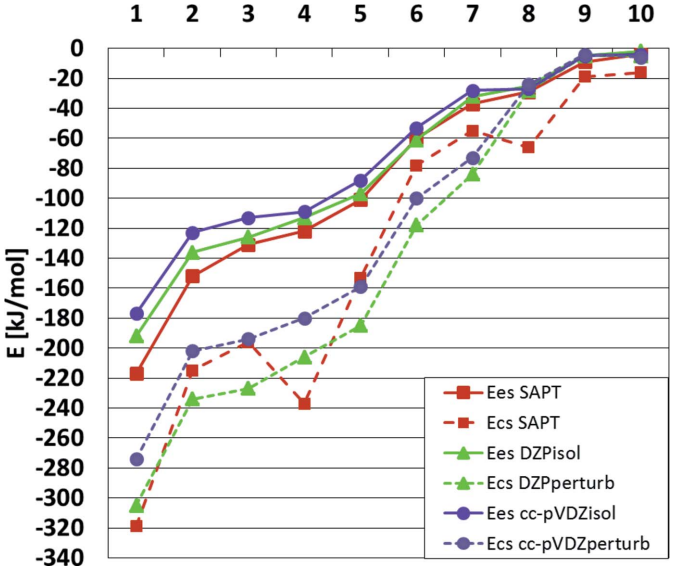

Figure 2
The Ees (kJ mol^{-1}) and Ecs (kJ mol^{-1}) values obtained on the basis of the theoretical electron densities, of either isolated (unperturbed) or perturbed molecules and from the DF–DFT–SAPT calculations (Ees = E^1_{pol}, Ecs = E^1_{pol} + E^2_{ind}) for the successive dimers of ALA and HIS. Dimers are ordered according to increasing values of Ees for the DZP_{isol} model.

3. Results and discussion

3.1. Interaction electron densities

Interaction electron densities were calculated by subtracting the electron-density models of the given isolated molecules from the corresponding perturbed electron-density models, using the same coordinates for each pair of electron-density models. Interaction densities obtained from theoretical models, DZP and cc-pVDZ, were not dependent on

parameters used to calculate maps, *e.g.* grid dimensions, and hardly change with basis sets used for the calculations (see Figs. 4*a* and 4*b*, and also the supplementary material[1]).

Without an electric field, the centres of a negative charge of electron orbitals coincide with the nuclei position. From interaction densities it seems that an external field breaks that symmetry, producing additional dipoles close to the nuclei. These dipoles occur in addition to aspherical densities at lone-pair and bonding regions. The phenomenon has been described in earlier studies (*e.g.* Czyznikowska *et al.*, 2009; Mitoraj *et al.*, 2010), but is also well represented by theoretical interaction densities obtained in our studies, for example positive and negative interaction densities of O atoms in ALA penetrate one another as chain rings (see Figs. 3*a*, 4*a* and the supplementary material). Mutual penetration of negative and positive interaction densities close to the positions of the nuclei is also observed for the histidine ring and peptide-bond atoms, which are involved in stronger intermolecular interactions (see Fig. 5 and the supplementary material). A similar shape of interaction densities was observed and described by Dittrich *et al.* (2012) for the non-standard amino acid L-homoserine.

The analysis of interaction densities obtained from theoretical electron densities and corresponding fits of the HC-MM (see Figs. 3, 4, 5 and 6) indicates that the shift of the electron cloud centre from the nuclei positions caused by an external field is not reproduced by the multipolar model. The reasons for this limitation of the HC-MM were described in detail by Koritsanszky *et al.* (2010), who showed that single Slater functions are not flexible enough to describe radial deformations. The frozen-core approximation used in the HC-MM leads to biased valence density parameters. Moreover, Koritsanszky *et al.* (2010) observed that radial signals, due to polarization of electrons localized in the vicinity of the nuclei, are extremely sharp and manifest themselves mainly in high-order reflections. Thus, it is hardly, if at all, possible to observe these signals using X-ray diffraction and the HC-MM. The Fourier truncation error is also manifested in the interaction densities presented here. Very high values of interaction densities are noticed at the positions of some nuclei in the case of fits of the HC-MM, whereas almost no density occurs in the same molecular fragments of corresponding purely theoretical densities (*e.g.* Figs. 5 and 6, histidine ring). However, interaction densities in lone-pair and bonding regions are well reproduced, at least qualitatively, by multipolar models based on theoretical densities.

Interaction densities occur mostly for molecular fragments directly involved in intermolecular interactions. Therefore, in some regions of the studied crystal structures the electron density is almost unchanged by the crystal environment (histidine ring in HA, methyl group in ALA, chain and ring C atoms in HIS). When the HC-MM is refined against experimental data, additional parameters have to be considered, *i.e.* thermal motions and scale factor. Consequently, obtaining the electron-density distribution from experimental data is more challenging. Therefore, we suggest a comparison of the interaction densities obtained from theoretical calculations with those obtained from experimental refinement, and verification as to whether interaction densities in both cases occur

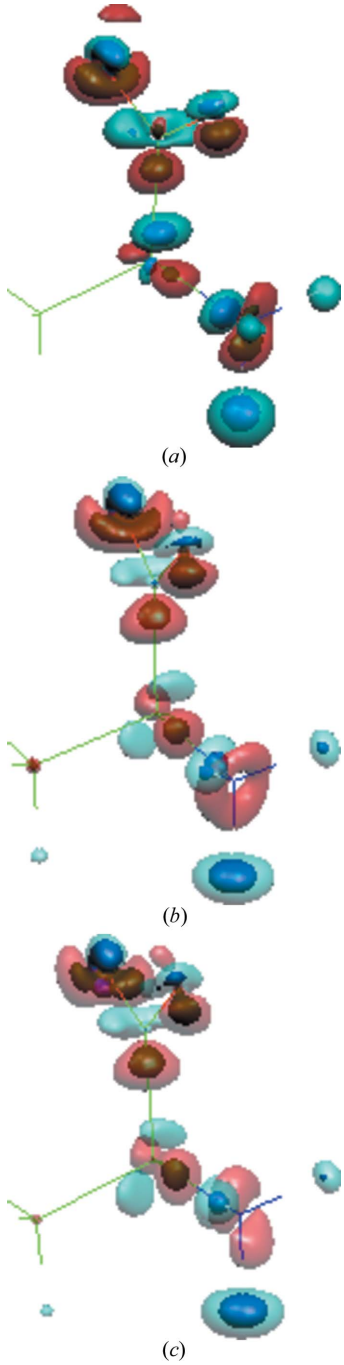

Figure 3
Three-dimensional interaction density maps (*Molekel* 4.3; Portmann, 2000–2002) for ALA, obtained with the use of the same atomic coordinates in all models: (*a*) $DZP_{perturb} - DZP_{isol}$, (*b*) $MM\_DZP_{perturb} - MM\_DZP_{isol}$, local symmetry constraints applied to multipolar parameters during refinement, (*c*) $MM\_DZP_{perturb} - MM\_DZP_{isol}$, all multipoles were refined for non-H atoms. Two isosurfaces are shown for each sign, positive: $\rho = 0.1$ e Å^{-3}, green, $\rho = 0.05$ e Å^{-3}, red; and negative: $\rho = 0.1$ e Å^{-3}, navy blue, $\rho = 0.05$ e Å^{-3}, blue.

[1] Supplementary material for this paper is available from the IUCr electronic archives (Reference: PC5013). Services for accessing these data are described at the back of the journal.

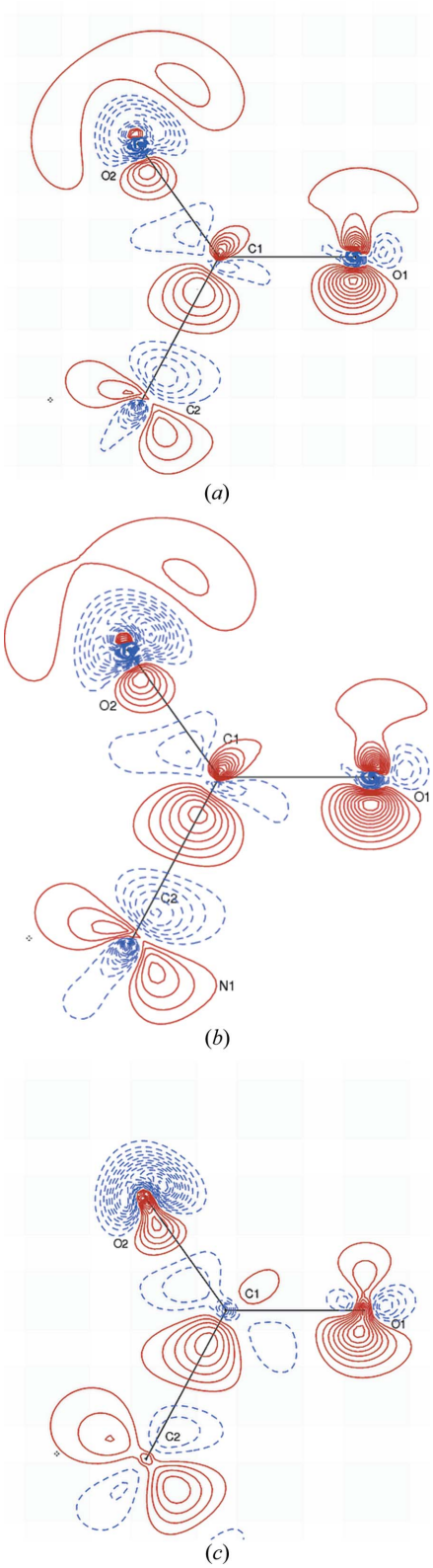

Figure 4
Two-dimensional interaction density maps for ALA in the plane of the carboxylic group, obtained from the theoretical and multipolar models, by subtracting isolated from perturbed electron-density models: (*a*) $DZP_{perturb} - DZP_{isol}$, (*b*) $cc\text{-}pVDZ_{perturb} - cc\text{-}pVDZ_{isol}$, (*c*) $MM\_DZP_{perturb} - MM\_DZP_{isol}$. The contour interval is equal to 0.025 e Å^{-3}, positive values are in red and negative values are in blue. Atomic coordinates were exactly the same in all models of a given molecule.

for the same molecular fragments. Such a comparison should indicate the influence of experimental errors or other inadequacies in refined experimental electron density.

3.2. Dipole moments

Molecular dipole-moment (DM) vectors were obtained either directly from theoretical density (DZP_{isol}, $DZP_{perturb}$) or from fits of the HC-MM (MM_DZP_{isol}, $MM\_DZP_{perturb}$). We extended the analysis of DM vectors by the results obtained in our earlier studies (Bąk *et al.*, 2011). Thus, DM vectors derived from multipolar models fitted to the crystal electron densities obtained in periodic calculations (CR) were additionally compared.

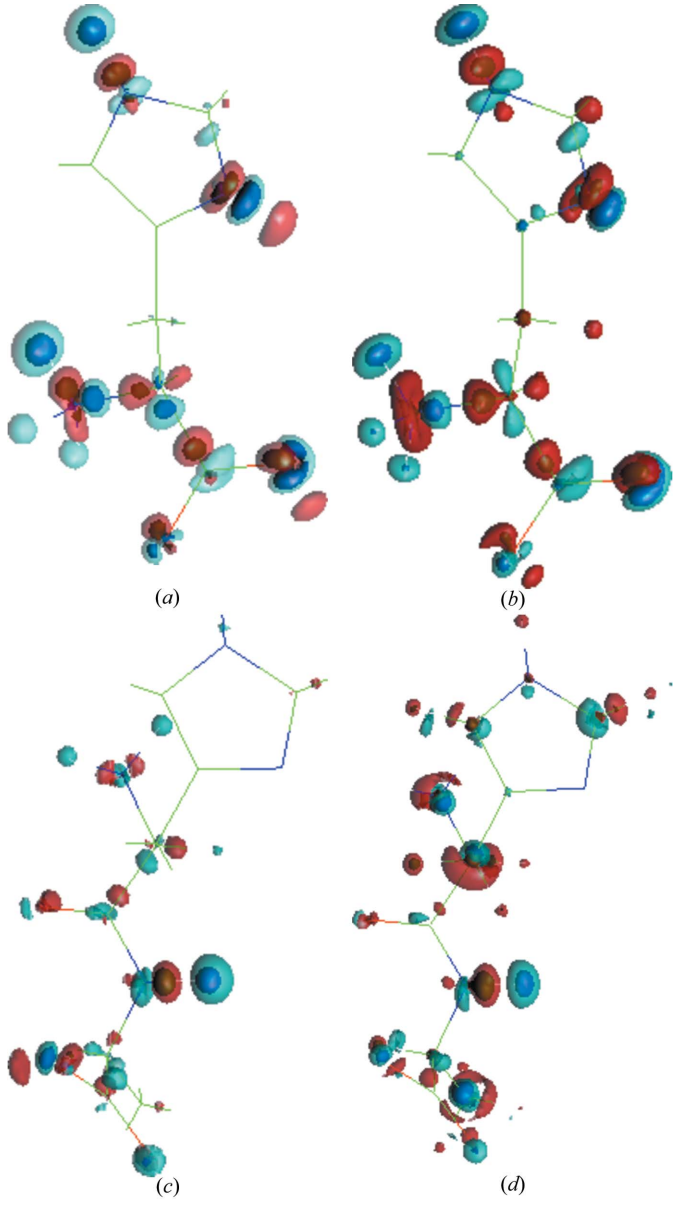

Figure 5
Three-dimensional interaction density maps of: (*a*) HIS from DZP models, (*b*) HIS from MM_DZP models, (*c*) HA from DZP models, (*d*) HA from MM_DZP models. Parameters of the isosurface are as for Fig. 3.

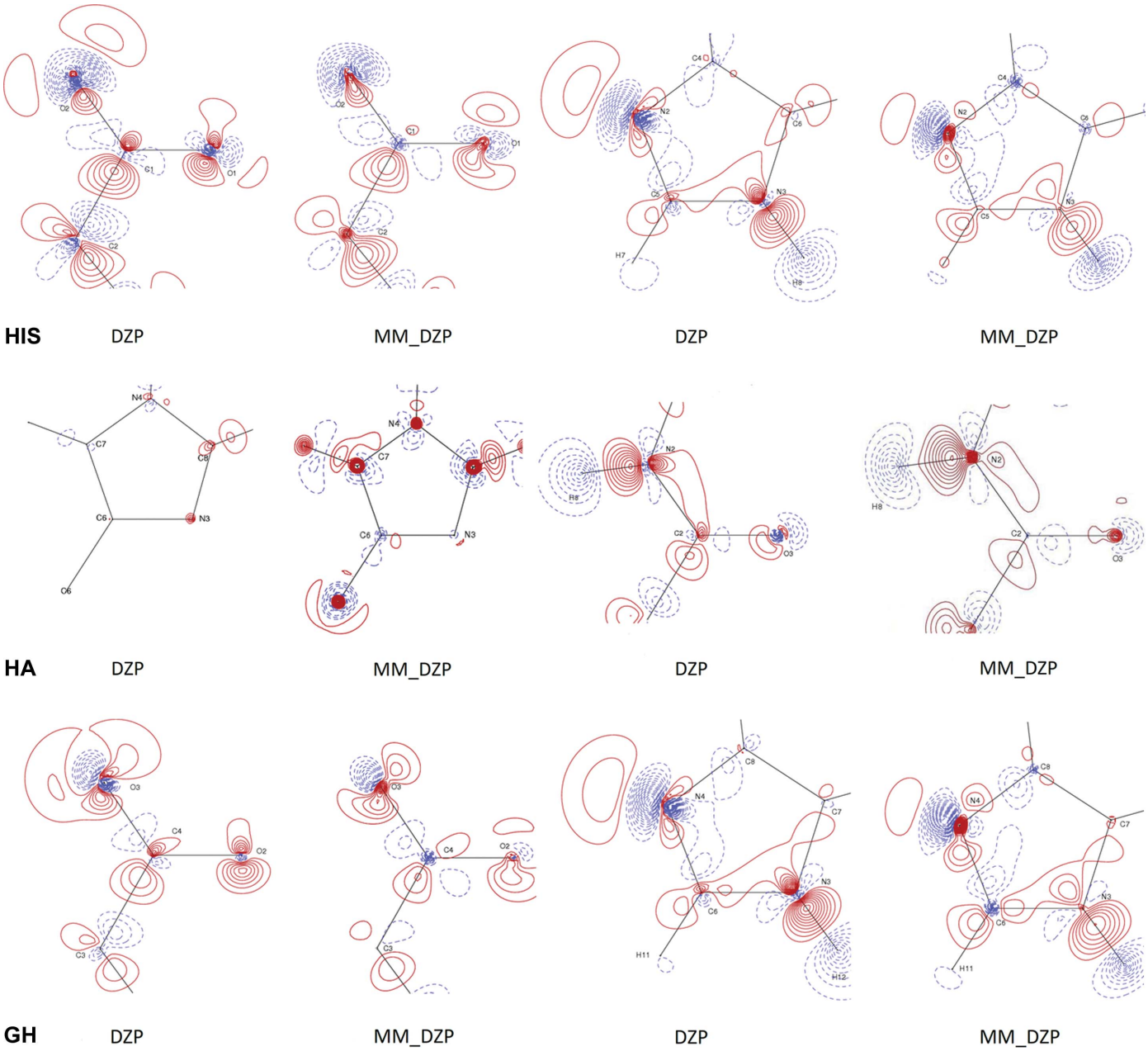

Figure 6
Two-dimensional interaction density maps. The parameters of the illustration are the same as for Fig. 4.

DM magnitudes derived from the perturbed densities ($DZP_{perturb}$) are much higher, up to 45%, than DM magnitudes obtained from the densities of isolated molecules (Table 3). Perturbation of the electron density due to the crystal environment also changed the directions of the DM vectors of the studied molecules up to 10° (Fig. 7). Since the method used for perturbation of the electron density takes into account only the electronic polarization effect, enhancement of DMs obtained from the $DZP_{perturb}$ models is likely to be larger than that induced by the real crystal environment. Nevertheless, DM magnitudes obtained from corresponding multipolar models of either theoretical perturbed densities or densities of isolated molecules are always underestimated (with the former being underestimated more) when compared with DMs derived from purely theoretical calculations. The DM magnitudes obtained from fits of the HC-MM to perturbed electron densities are similar to the results obtained directly from theoretical electron densities of isolated molecules. More important, the enhancement of DMs caused by the polarization of electron density is hardly seen in the case of fits of the HC-MM model (Table 3 and Fig. 7). The dipole moments obtained from multipolar models of electron densities of the crystal (CR) seem to be more similar to the DM derived from multipolar models of perturbed densities ($MM\_DZP_{perturb}$; Table 3; Fig. 7).

Table 3
Molecular dipole-moment magnitudes (D).

	DZP_{isol}	$DZP_{perturb}$	Δ%†	MM_DZP_{isol}	$MM\_DZP_{perturb}$	Δ%	CR
ALA	11	16	45%	8	10	22%	11
HIS	14	22	55%	11	14	27%	12
HA	24	26	8%	23	22	−4%	23
GH	22	30	36%	18	21	16%	19

† Δ% enhancement of DM magnitude.

Spackman *et al.* (1999) and Dittrich *et al.* (2012) also studied the ability of the multipolar model to reproduce DM magnitudes of isolated molecules and molecules in crystals. They obtained analogous trends between DM magnitudes calculated directly from theoretical and multipolar model electron densities to those shown in our study.

3.3. Coulombic interaction energy

We also analysed intermolecular Coulombic energies of interactions in 17 dimers (see Tables S1 and S2 in the supplementary material). These were calculated directly from successive pairs of theoretical electron densities of either perturbed (Ecs) or isolated molecules (Ees). As mentioned before, it was assumed that the Ecs values calculated from the perturbed electron-density models correspond to the sum of electrostatic and induction energy components as defined in the SAPT methods. The results obtained from multipolar models of theoretical perturbed densities ($MM\_DZP_{perturb}$, $MM\_cc\text{-}pVDZ_{perturb}$) were referred to Ecs values calculated directly from theoretical perturbed electron densities ($DZP_{perturb}$ and $cc\text{-}pVDZ_{perturb}$). Additionally, values of Ecs derived from the multipolar model of crystal electron density obtained from B3LYP/DZP periodic calculations (Bąk *et al.*, 2011) were included in the analyses (CR). We studied the trends in differences which occurred between Ecs and Ees values obtained directly from theoretical electron densities and checked whether they are reproduced by multipolar models of electron densities. Energy values for ALA and HIS dimers, which represent differences between Ees and Ecs energies in all studied molecules, are presented in Fig. 8.

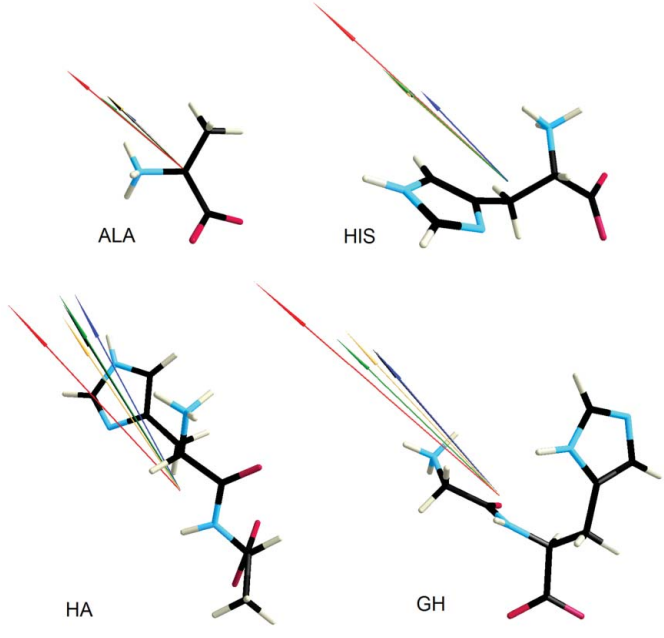

Figure 7
The *MolecoolQt* (Hübschle, 2010) representations of the molecular dipole-moment vectors obtained either directly from the wavefunctions or from multipolar models. The colours of the vectors indicate particular models: red, $DZP_{perturb}$; yellow, $MM\_DZP_{perturb}$; green, DZP_{isol}; blue, MM_DZP_{isol}; black, CR.

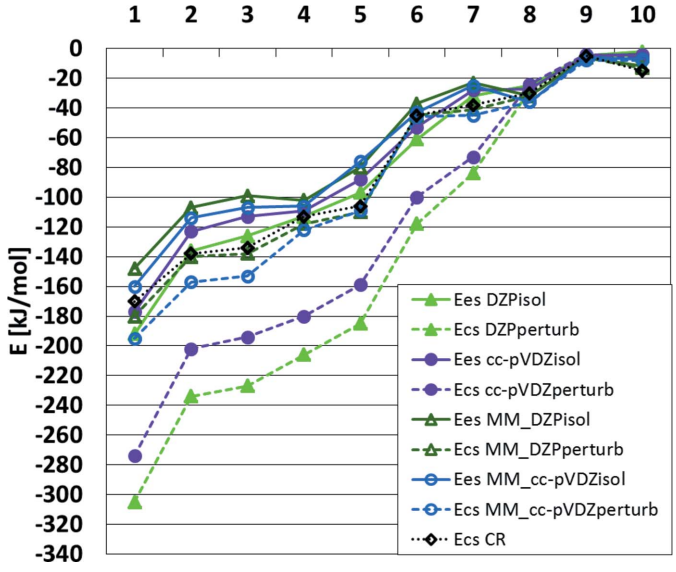

Figure 8
The Ees (kJ mol^{-1}) and Ecs (kJ mol^{-1}) values obtained directly from the theoretical electron densities of either isolated or perturbed molecules, and from the fits of the HC-MM model to respective theoretical electron densities for the successive dimers of ALA and HIS. Results obtained from the CR periodic density model are also presented. Dimers are ordered according to increasing values of Ees for the DZP_{isol} model.

The fits of the HC-MM to the perturbed theoretical densities do not reproduce Ecs values obtained directly from the theoretical electron densities. RMSDs calculated between Ecs values derived from purely theoretical perturbed density models and from corresponding multipolar models are 73 and 44 kJ mol^{-1} in the case of DZP and cc-pVDZ basis sets, respectively (see Table 4). A much better situation is observed in the case of isolated-molecule densities and Ees values. RMSDs between Ees values computed directly from theoretical densities and those derived from corresponding multipolar models are 22 and 9 kJ mol^{-1} for DZP and cc-pVDZ basis sets, respectively. Furthermore, the values of Ecs computed from the multipolar models of perturbed densities (or crystal densities, CR) are much closer to the Ees values obtained directly from isolated-molecule densities (10 and 20 kJ mol^{-1} for DZP and cc-pVDZ basis sets, respectively) than to the Ecs values from referential perturbed densities. Consequently, trends which occur in differences between Ecs and Ees values computed from theoretical models (DZP_{isol}

Table 4
RMSDs calculated between intermolecular interaction energy values (kJ mol^{-1}) obtained from successive pairs of studied models.

The statistics taking into account results obtained from ten dimers of ALA and HIS are given together with the ones based on all 17 dimers of four crystal structures (numbers in parentheses).

	Ees MM_DZP$_{isol}$	Ecs MM_DZP$_{perturb}$	Ees MM_cc-pVDZ$_{isol}$	Ecs MM_cc-pVDZ$_{perturb}$
Ees DZP$_{isol}$	22 (19)	10 (17)		
Ecs DZP$_{perturb}$	95 (98)	73 (73)		
Ees cc-pVDZ$_{isol}$			9	20
Ecs cc-pVDZ$_{perturb}$			68	44
Ees MM_DZP$_{isol}$		23 (26)		
Ees MM_cc-pVDZ$_{isol}$				26
Ecs CR	19 (18)	4 (13)	16	13

and DZP$_{perturb}$ or cc-pVDP$_{isol}$ and cc-pVDZ$_{perturb}$) are not fully reproduced by the results of the multipolar models.

We have to admit that Ecs values in the case of multipolar models are always more negative than (or in some cases equal to) the corresponding values of Ees. However, the differences between Ees and Ecs values for multipolar models (RMSD = 23 and 26 kJ mol^{-1} for MM_DZP and MM_cc-pVDZ difference, respectively) are much smaller than those observed for values computed directly from theoretical densities (about 65 kJ mol^{-1}, see Tables 1 and 4). In addition, a systematic increase of difference between Ees and Ecs values with increasing strength of interaction is hardly seen for energies obtained from multipolar models.

Ecs values obtained from fits of the HC-MM to perturbed electron densities from cluster calculations are almost the same as those obtained from fits of the HC-MM to periodic *ab initio* calculations in which the same DZP basis set was used (RMSD = 4 kJ mol^{-1}, see Table 4).

4. Conclusions

Cluster calculations were used for perturbation of the theoretical density of single molecules in their crystal environment. Electron densities and electrostatic properties such as dipole moments and Coulombic electrostatic interaction energies were derived from unperturbed (isolated-molecule) and perturbed electron densities of the molecules. Subsequently, for all the properties, differences between corresponding values caused by perturbation of the electron density were established. The differences between Coulombic interaction energies obtained from perturbed and unperturbed theoretical electron densities were compared to the induction energy values obtained from the DF–DFT–SAPT calculations. This verified the credibility of the applied cluster perturbation method. Then, the ability of the Hansen–Coppens multipolar model (HC-MM) to properly describe the electron density and electrostatic properties of molecules in crystals was studied in reference to the theoretical electron densities obtained in the cluster calculations.

Our results indicate that the multipolar model is not able to reproduce the influence of the crystal environment on the dipole moment and interaction energy values. The multipolar model approximately describes the electrostatic properties of isolated molecules, with an error in electrostatic interaction energies of about 15 kJ mol^{-1}, whereas the error of the multipolar model in estimation of electrostatic properties computed from perturbed densities (about 60 kJ mol^{-1} for interaction energies) is of the same magnitude as the polarization effect itself (about 65 kJ mol^{-1} for interaction energies). Electrostatic properties approximated by the multipolar model of perturbed theoretical densities resemble more closely isolated-molecule properties than those of molecules in the crystal environment, both derived directly from theoretical densities.

Even if we do not consider absolute values of electrostatic properties but focus only on relative values (differences between perturbed and unperturbed density properties), these are also not reproduced reliably by the multipolar model. Firstly, results obtained from multipolar models suggest that the effect of polarization is much smaller. Secondly, in the case of Coulombic interaction energy, they do not reproduce the trend: the stronger the electrostatic interaction between unperturbed densities, the larger is the effect of perturbation on interaction energy.

The failure of the HC-MM in reproducing electrostatic properties, *e.g.* dipole moment and interaction energy, of molecules in the crystal seems to be connected with an inadequate description of electron density close to the nuclear positions. The main difference in the description of interaction densities between theoretical electron densities and fits of the HC-MM corresponding to these densities occurs in the vicinity of the nuclei. An external field shifts the centre of a negative charge of valence electron orbitals from the nuclei position, producing additional dipoles at these positions. This effect is manifested in interaction densities derived from theoretical electron densities and is not reproduced by fits of the HC-MM. Electron density in bonding and lone-electron-pair regions is reproduced qualitatively by the HC-MM. It appears that the ability to describe properly sharp features close to nuclei is not so crucial for modelling the electron density of isolated molecules.

To sum up, we have to conclude that the HC-MM model fitted in Fourier space is not able to *quantitatively* reproduce interaction densities as well as enhancements of molecular dipole moments and Coulombic interaction energies caused by the crystal environment.

PMD is grateful for the support received from the Foundation for Polish Science with the POMOST/2010–2/3 project co-financed by the European Union, Regional Development Fund. JMB and PMD would like to thank Anatoliy Volkov for providing the authors with the *SPDFG* program. ZC is

grateful for the CPU time in the Wroclaw Center of Networking and Supercomputing (WCSS).

References

Bąk, J. M., Domagała, S., Hübschle, C., Jelsch, C., Dittrich, B. & Dominiak, P. M. (2011). *Acta Cryst.* A**67**, 141–153.

Becke, A. D. (1993). *J. Chem. Phys.* **98**, 5648–5652.

Chambrier, M. H., Bouhmaida, N., Bonhomme, F., Lebegue, S., Gillet, J. M., Jelsch, C. & Ghermani, N. E. (2011). *Cryst. Growth Des.* **11**, 2528–2539.

Clementi, E. & Raimondi, D. L. (1963). *J. Chem. Phys.* **38**, 2686–2689.

Clementi, E. & Roetti, C. (1974). *At. Data Nucl. Data Tables*, **14**, 177–478.

Coppens, P., Dam, J., Harkema, S., Feil, D., Feld, R., Lehmann, M. S., Goddard, R., Krüger, C., Hellner, E., Johansen, H., Larsen, F. K., Koetzle, T. F., McMullan, R. K., Maslen, E. N. & Stevens, E. D. (1984). *Acta Cryst.* A**40**, 184–195.

Czyznikowska, Z., Lipkowski, P., Góra, R. W., Zaleśny, R. & Cheng, A. C. (2009). *J. Phys. Chem. B*, **113**, 11511–11520.

Destro, R., Soave, R. & Barzaghi, M. (2008). *J. Phys. Chem. B*, **112**, 5163–5174.

Dittrich, B., McKinnon, J. J. & Warren, J. E. (2008). *Acta Cryst.* B**64**, 750–759.

Dittrich, B., Sze, E., Holstein, J. J., Hübschle, C. B. & Jayatilaka, D. (2012). *Acta Cryst.* A**68**, 435–442.

Dominiak, P. M., Volkov, A., Dominiak, A. P., Jarzembska, K. N. & Coppens, P. (2009). *Acta Cryst.* D**65**, 485–499.

Dovesi, R., Causa, M., Orlando, R., Roetti, C. & Saunders, V. R. (1990). *J. Chem. Phys.* **92**, 7402–7411.

Dunning, T. H. (1970). *J. Chem. Phys.* **53**, 2823–2833.

Dunning, T. H. (1989). *J. Chem. Phys.* **90**, 1007–1023.

Fournier, B., Bendeif, el-E., Guillot, B., Podjarny, A., Lecomte, C. & Jelsch, C. (2009). *J. Am. Chem. Soc.* **131**, 10929–10941.

Grabowsky, S., Pfeuffer, T., Morgenroth, W., Paulmann, C., Schirmeister, T. & Luger, P. (2008). *Org. Biomol. Chem.* **6**, 2295–2307.

Hansen, N. K. & Coppens, P. (1978). *Acta Cryst.* A**34**, 909–921.

Hathwar, V. R., Thakur, T. S., Guru Row, T. N. & Desiraju, G. R. (2011). *Cryst. Growth Des.* **11**, 616–623.

Hesselmann, A., Jansen, G. & Schütz, M. (2005). *J. Chem. Phys.* **122**, 014103.

Holstein, J. J., Luger, P., Kalinowski, R., Mebs, S., Paulman, C. & Dittrich, B. (2010). *Acta Cryst.* B**66**, 568–577.

Hübschle, C. B. (2010). *MoleCoolQt* – a molecule viewer for charge density related science, http://www.molecoolqt.de. Georg-August-University Gottingen, Germany.

Jayatilaka, D. & Grimwood, D. J. (2003). *Computational Science – ICCS 2003*, **2660**, 142–151.

Jayatilaka, D., Munshi, P., Turner, M. J., Howard, J. A. & Spackman, M. A. (2009). *Phys. Chem. Chem. Phys.* **11**, 7209–7218.

Koritsanszky, T., Volkov, A. & Chodkiewicz, M. (2010). Editors. *Structure and Bonding*, Vol. 147, pp. 1–25. Berlin: Springer-Verlag.

Lee, C., Yang, W. & Parr, R. (1988). *Phys. Rev. B*, **37**, 785–789.

Liebschner, D., Elias, M., Moniot, S., Fournier, B., Scott, K., Jelsch, C., Guillot, B., Lecomte, C. & Chabrière, E. (2009). *J. Am. Chem. Soc.* **131**, 7879–7886.

Madsen, G. K., Krebs, F. C., Lebech, B. & Larsen, F. K. (2000). *Chem. Eur. J.* **6**, 1797–1804.

Mitoraj, M. P., Kurczab, R., Boczar, M. & Michalak, A. (2010). *J. Mol. Model.* **16**, 1789–1795.

Munshi, P., Jelsch, C., Hathwar, V. R. & Guru Row, T. N. (2010). *Cryst. Growth Des.* **10**, 4670.

Portmann, S. (2000–2002). CSCS/ETHZ Switzerland (original IRIX GL implementation, by Peter F. Fluekiger, CSCS/UNI Geneva).

Spackman, M. A. & Byrom, P. G. (1996). *Acta Cryst.* B**52**, 1023–1035.

Spackman, M. A., Byrom, P. G., Alfredsson, M. & Hermansson, K. (1999). *Acta Cryst.* A**55**, 30–47.

Volkov, A., King, H. F. & Coppens, P. (2006). *J. Chem. Theory Comput.* **2**, 81–89.

Volkov, A., Macchi, P., Farrugia, L. J., Gatti, C., Mallinson, P., Richter, T. & Koritsanszky, T. (2006). *XD2006.* Middle Tennessee State University, USA, Universita di Milano and CNR-ISTM Milano, Italy, University of Glasgow, Scotland, State University of New York at Buffalo, USA, and Freie Universitat Berlin, Germany.

Volkov, A., Messerschmidt, M. & Coppens, P. (2007). *Acta Cryst.* D**63**, 160–170.

Werner, H. J. *et al.* (2006). *Molpro*, version 2006.1. http://www.molpro.net.

Zarychta, B., Pichon-Pesme, V., Guillot, B., Lecomte, C. & Jelsch, C. (2007). *Acta Cryst.* A**63**, 108–125.